Fracture 1977, Volume 2, ICF4, Waterloo, Canada, June 19 -24, 1977

CORRELATIONS BETWEEN CRACK INITIATION, PROPAGATION AND MICROSTRUCTURE IN A MEDIUM STRENGTH Cr-Mo-V STEEL

H. Kotilainen and K. Törrönen*

INTRODUCTION

Good toughness can generally be achieved in low-alloy steels by grain refinement. The yield and cleavage fracture strength can be estimated in such cases by using the Hall-Petch relationship. The purposes of alloying are thus to prevent grain growth and also to increase hardenability. If alloying gives rise to secondary hardening a good strength can be achieved even with coarse grain size, but then the fracture behaviour becomes rather complicated.

BASIS OF THE WORK

The aim of the present work was to examine and evaluate the fracture behaviour of a Cr-Mo-V steel (2.8% Cr, 0.6% Mo, 0.3% V and 0.18%C), which was quenched and tempered to a Hollomon-Jaffe tempering parameter value of about 20100. The Charpy V and fracture toughness tests, which both measure the resistance to crack initiation, indicated very good toughness (Figure 1). Also the estimates for dynamic fracture toughness K_{Id} made by instrumented impact tests or according to the method proposed by Barsom and Rolfe [1] were at least moderately good. In contrast the Pellini drop-weight test gave a remarkably high value (293 K) for the NDT-temperature as compared to the steeply rising part of the fracture toughness curve or to the impact energy curve (CVE), which reaches the upper shelf energy value (100% shear) at a lower temperature than the NDTT. The results of the dynamic tear test (DTE) confirmed further the very high propagation transition temperature, as the 50% METT proved to be 333 K. The big difference between initiation and propagation transitions cannot be explained solely on the basis of different deformation speeds during testing, as is evident when comparing the K_{Ic} and K_{Id}-curves and NDTT. Instead the explanation must be sought from the microstructure.

EXPERIMENTAL PROCEDURE AND RESULTS

Mechanical Tests

The results of the mechanical tests are given in Figure 1. The fracture toughness K_{Ic} has been measured according to ASTM E399-74 using CT-specimens 25, 50 and 100 mm thick. The NDT-temperature was determined according to ASTM E208-69 using both P-1 and P-3 specimens. The DT-specimens were 300 mm thick and their width was 75 mm. The machined notch was 25 mm deep and sharpened by pressing with a knife ($\rho \leq 0{,}02$ mm). Standard Charpy V specimens with a knife pressed notch were used for instrumented impact tests.

*Technical Research Centre of Finland, Reactor Materials Research, SF-02150 ESPOO 15, Finland.

Microstructure

The microstructure consisted of tempered granular bainite. Grain sizes were estimated using transmission electron and optical microscopy. The prior austenite grain size was ASTM 3 (127 μm), the ferrite grain size 44 μm and the lath packet width 1,33 μm (mean value of several samples, the mean values of which varied between 0,9 and 1,9 μm). The lath width was 0,43 μm [2]. The microstructural parameter which controls the strength is, however, a fine dispersion of vanadium rich MC-type carbides. The planar interparticle distance and the size of these carbides determines the yield strength of the studied steel according to the Orowan relation [3]. The mean size D of the squared plate shaped MC-carbides was 14,2 nm and the planar interparticle spacing L_A = 0.131 μm[2].

The yield strength of the steel as well as the Charpy V transition temperatures and NDT-temperature are linearly related to the inverse of a parameter λ, which is defined as [3]

$$\lambda^{-1} = \left(L_A - D \right)^{-1} \ln \frac{D}{b} \qquad (1)$$

DISCUSSION

Crack Nucleation and Initial Growth

An estimate for the fracture stress required for microcrack nucleation and initial growth can be obtained by using the Griffith equation [4]

$$\sigma_{fG} = \left[\frac{4E\gamma_p}{\pi(1-\nu^2)d} \right]^{1/2} \qquad (2)$$

By substituting d with various measured grain sizes and carbide spacings and by using γ_p = 1.5 Jm^{-2} [5], the values given in Table 1 were obtained. If we compare the values in Table 1 to the information in Figure 2, which gives the yield and fracture stress as a function of MC-carbide spacing [3], it is seen that the fracture stress values calculated by carbide spacing and lath width are too high. As the value for fracture stress (790 MPa) which can be obtained from Figure 2 is higher than the value calculated by using lath packet width as d, and as it is also higher than the corresponding yield stress, some plastic deformation and work hardening is needed to raise the stress to such a level that crack nucleation and initial growth occurs.

By using instrumented impact testing, the fracture stress could also be calculated by the following equation after the method of Green and Hundy [6]

$$\sigma_f = \frac{P_f \cdot S}{1{,}45B(W-a)^2} \qquad (3)$$

where P_f is the force at fracture, S is span width and W the specimen width. When the results of the tests (Figure 3) were substituted into equation (3), it was observed that σ_f = 850 MPa, which is in rather good agreement with the value obtained from Figure 2. This value can be considered to be the maximum value for crack initiation.

This result confirms that the fracture stress values calculated using the carbide spacing or lath width in equation (2) are hypothetical and too high. The lath packet width, instead, seems to be the smallest unit restricting the initial crack growth. Thus high-angle boundaries are strong enough obstacles to stop microcracks, while small carbides or low-angle lath boundaries are not. This same result is obtained by studying the fracture surfaces, on which a cleavage fracture unit size of 2.3 μm has been measured [3]. The crack nucleation and initial growth is very difficult because a fine dispersion of carbides restricts the necessary strain hardening and dislocation pile-up length. When a microcrack, however, has been nucleated, a relaxation of internal stresses introduced by piled-up dislocations occurs. This apparently makes the deformation easier inside a single lath packet, and consequently such a microcrack may not be critical.

Several non-propagating microcracks may thus be initiated. This explains that also under impact loading the crack initiation is difficult. The stress should increase up to the cleavage fracture stress 1200 MPa, in order that the first microcrack would be critical. This value for cleavage fracture stress is achieved when the tensile test results are extrapolated down to 60 K. This stress is so much higher than the fracture stress (Figure 2) that the initiation of a stable microcrack is probable assuming that the cleavage fracture stress is rather temperature independent.

The good toughness which the studied Cr-Mo-V steel exhibits against crack initiation is thus due to both a fine carbide dispersion, which effectively restricts plastic deformation, and also to small width of lath packets, the boundaries of which can arrest growing microcrack. The good toughness prevails also in a notched structure providing the temperature is high enough to keep the difference $\sigma_f - \sigma_y$ big enough.

Crack Propagation

A prerequisite for crack propagation is that microcracks can traverse the lath packet boundary. The surface energy of traversing the boundary γ_B determines the required stress. To a first approximation this stress can be assumed to be equal to the cleavage fracture stress, which can be achieved only after excessive strain hardening. Apparently some microcrack joining is also needed. When the stress required to traverse the high-angle boundary of a lath packet has been achieved, the crack propagates easily under the stress of 573 MPa, which is calculated according to equation (2) for average lath packet width. The traversing of the boundary is apparently a fast process due to high stored elastic energy. After this critical step the slowing and arresting of the propagating microcrack depends on the possibilities for plastic deformation at the crack tip. The dislocations, however, are tightly locked by a fine carbide dispersion, and thus the crack can propagate further without losing its speed. Thus the benefit of a fine carbide dispersion in raising the stress required for crack initiation has become a disadvantage when considering crack propagation.

When the propagating crack meets the following high-angle boundary, whether it is lath packet, ferrite or austenite grain boundary, the speed of the crack is still high. As the crack length has also increased, it is possible that the crack continues to propagate, even if the γ_B is large. Further evidence of low propagation resistance has been obtained in a fatigue test, which was conducted at room temperature at 0.5 Hz frequency using 50 mm thick CT-specimen. An unstable fracture occurred at K_C = 185 MPa $m^{1/2}$, and the fracture surface was totally plain without any shear lips [7].

The initiation of a crack was shown to be controlled by both the interparticle spacing of carbides and the lath packet width. The crack propagation is, instead, controlled only by carbide spacing, which in turn directly determines the ease of plastic deformation. This indicates that the NDT-temperature should be linearly related to the inverse of the carbide spacing, as has been observed [3].

The great difference between crack initiation and propagation behaviours can also be examined by using the method proposed by Tetelman [8]. The energy γ_p opposing the crack propagation depends among other things on the crack velocity and temperature. At constant temperature the increase of crack velocity produces an exponential decrease of γ_p. This corresponds well with dislocation locking by fine carbides in the present steel. As the number of dislocation sources is small also due to carbides, the absolute value of γ_p may be rather small. Only a considerable increase in the temperature improves the dislocation mobility and hence plastic deformation, which increase the value of γ_p. The situation is illustrated in Figure 4. When the crack velocity has achieved a constant value, the propagation continues until the arrest stress intensity factor K_a has been reached or the component breaks.

The behaviour explained above is different from the behaviour of "Petch-materials", the grain size of which controls both the yield and cleavage fracture strength [9]. In "Petch-materials" intergranular plastic deformation is easy when the value of γ_p is large. In this case the initiation of a microcrack is difficult, as in the studied Cr-Mo-V steel, but for a different reason. The actual difference between these steel types arises, however, when the microcrack traverses the first grain boundary. As local plastic deformation is easy in "Petch-material", there exists no such pop-in as in the Cr-Mo-V steel. As the deformation is easy around the tip of propagating crack, the value of γ_p does not decrease as much as in Cr-Mo-V steel. This behaviour of "Petch-material" enables the crack to be arrested even at the second grain boundary, and thus there does not exist such a large difference between crack initiation and propagation as in the studied Cr-Mo-V steel.

CONCLUSIONS

In quenched and tempered secondary hardening Cr-Mo-V steel the crack initiation is controlled by a fine carbide dispersion and by the high-angle boundary of the lath packet inside which the crack has nucleated. The crack propagation, however, is determined only by the carbide dispersion. This behaviour accomplishes good toughness against crack initiation even in dynamic testing. Thus the crack propagation behaviour cannot be examined according to K_{Id} values. When the crack starts to grow instably, there are no strong microstructural barriers opposing the propagation due to the carbide strengthened matrix.

When evaluating the toughness of the Cr-Mo-V steel, one must clearly distinguish between fracture initiation and fracture propagation. The fracture behaviour of the studied Cr-Mo-V steel differs essentially from the behaviour of those steels whose strength and toughness has been achieved by grain refinement. This is seen also in the fact that the yield and cleavage fracture stress of the Cr-Mo-V steel does not obey the Hall-Petch relationship.

ACKNOWLEDGEMENTS

We are grateful to Dr. Jarl Forstén for his continuous interest and valuable discussions in every stage of this research. This work was done under the auspices of the Ministry of Trade and Industry. The financial support of the Eemil Aaltonen Foundation and Suomen Kulttuurirahasto (K.T.) is also gratefully acknowledged.

REFERENCES

1. BARSOM, J. M. and ROLFE, S. T., Engng Fracture Mech., 2, 1971, 341.
2. TÖRRÖNEN, K. To be published.
3. TÖRRÖNEN, K. and KOTILAINEN, H., II-69-H, ICF 4, Waterloo, 1977.
4. GRIFFITH, A. A., Phil. Trans. Roy. Soc., London, A 221, 1920, 163.
5. HAHN, G. T. and ROSENFIELD, A. R., Acta Met., 14, 1966, 1815; Trans. Met. Soc., AIME, 239, 1967, 668.
6. GREEN, A. P. and HUNDY, B. B., J. Mech. Phys. Solids, 4, 1956, 128.
7. RAHKA, K., Private communication, 1975.
8. TETELMAN, A. S., Fracture of Solids, Interscience, New York, 1963, 461.
9. PETCH, N. J., J. Iron Steel Institute, 174, 1953, 25.

Table 1 Estimated Fracture Stresses for Different Microstructural Units

Microstructural Unit	d (μm)	σ_{fG} (MPa)
Carbide spacing	0,131	1825
Lath width	0,43	1008
Lath packet width min	0,90	696
Lath packet width mean	1,33	573
Lath packet width max	1,90	479
α-grain size	44	100
γ-grain size	127	59

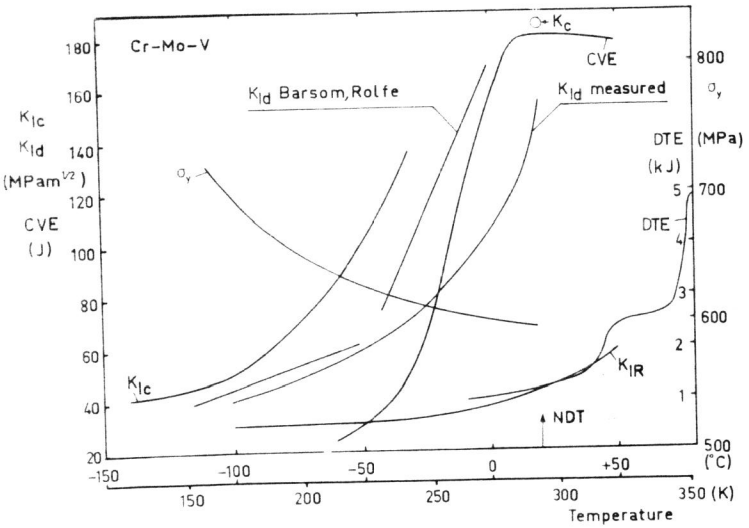

Figure 1 Temperature Dependence of Mechanical Properties of Cr-Mo-V Steel, (DTE Dynamic Tear Energy, CVE Charpy V Energy)

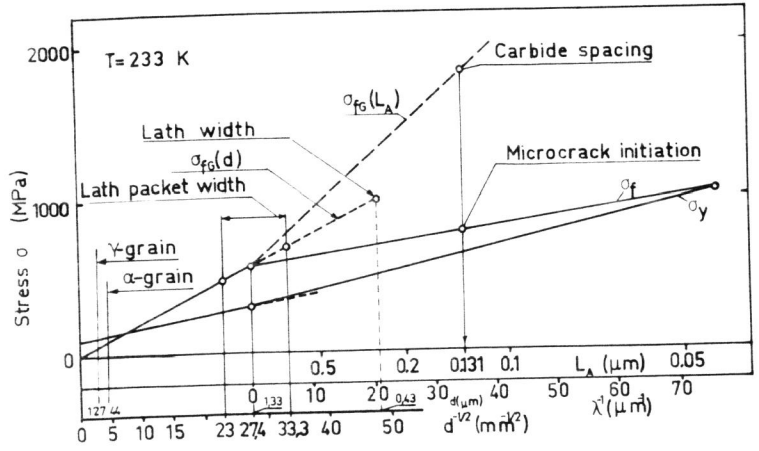

Figure 2 Dependence of Fracture Stress σ_f and Yield Stress σ_y on Microstructural Units, d (sub)grain size, L_A carbide spacing.

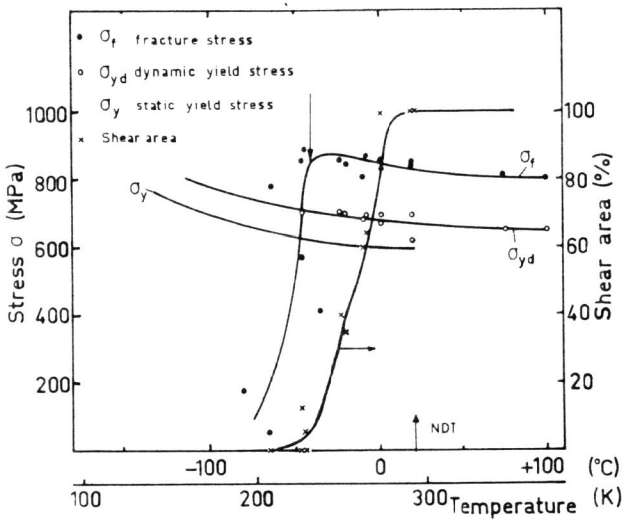

Figure 3 Results of Instrumented Impact Test

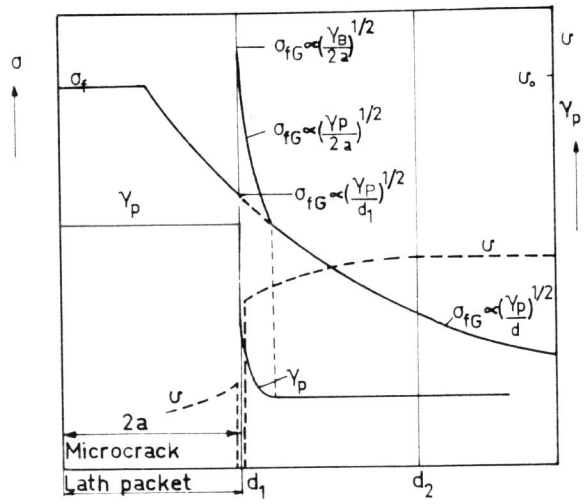

Figure 4 Schematic Diagram of the Pop-In of a Microcrack Through a High-Angle Boundary